scientific reports

OPEN

Prognostic implications of quantitative flow ratio and optical coherence tomography-guided neointimal characteristics in drug-coated balloon treatment for in-stent restenosis

Shiwan Lu[1,3], Li Pan[1,3], Ning Gu[1,3], Yi Deng[1], Chancui Deng[1], Xiushi Li[1], Feng Wang[1], Yongchao Zhao[1], Zhenglong Wang[2✉] & Bei Shi[1✉]

The aim of this study was to investigate the relationship between quantitative flow ratio (QFR) after drug-coated balloon (DCB) treatment for in-stent restenosis (ISR) and between neointimal characteristics assessed by optical coherence tomography (OCT) and clinical outcomes. This single-center, retrospective, observational cohort study included ISR patients who underwent DCB angioplasty under OCT guidance. The primary outcome of the study was a target vessel failure (TVF), defined as a composite endpoint of cardiovascular death, target vessel myocardial infarction and target vessel revascularization. During a median follow-up of 756 days (IQR: 443.25, 1134.50), 204 ISR patients underwent OCT-guided DCB angioplasty, resulting in TVF development in 27 patients. At the post-procedural DCB angioplasty, the vessel-level QFR was significantly lower in the TVF group (0.89 [IQR: 0.87, 0.93] vs. 0.93 [IQR: 0.91, 0.96]; $P < 0.001$) than in the non-TVF group. Analysis of the qualitative characteristics of ISR lesions showed a significantly higher incidence of heterogeneous neointima in the TVF group compared with the non-TVF group (13 [48.15%] vs. 32 [18.08%]; $P < 0.001$). In the multivariable Cox regression analysis, low vessel-level QFR (HR per 0.1 increase: 0.11; 95% CI: 0.03–0.41; $P < 0.001$) and heterogeneous neointima were independently associated with TVF. The TVF rate of vessels with the 2 features was 10.69 times higher than that of all other vessels (95%CI [2.05–55.79]; log-rank $P < 0.0001$). Vessel-level QFR and heterogeneous neointima were independent factors associated with TVF in ISR patients after DCB angioplasty. Adding the QFR measure-ment to OCT findings may enable better discrimination of patients with subsequent TVF post-DCB angioplasty for ISR.

Keywords In-stent restenosis (ISR), Drug-coated balloon (DCB), Quantitative flow ratio (QFR), Optical coherence tomography (OCT)

Abbreviations

ARC	Academic Research Consortium
AUC	Area under the curve
CAG	Coronary angiography
CI	Confidence interval
DCB	Drug-coated balloon
DES	Drug-eluting stents

[1]Department of Cardiology, Affiliated Hospital of Zunyi Medical University, No. 149 Dalian Road, Huichuan District, Zunyi City 563000, Guizhou, China. [2]Department of Cardiology, The Third Affiliated Hospital of Zunyi Medical University, No. 98 Fenghuang North Road, Xima Road Street, Huichuan District, Zunyi City 563002, Guizhou, China. [3]Shiwan Lu, Li Pan and Ning Gu contributed to this work equally. ✉email: wangzhenglong321@163.com; shib@zmu.edu.cn

FFR	Fractional flow reserve
HR	Hazard ratio
IQR	Interquartile range
ISNA	In-stent neoatherosclerosis
ISR	In-stent restenosis
OCT	Optical coherence tomography
OR	Oddis ratio
PCI	Percutaneous coronary interventions
QCA	Quantitative coronary angiography
QFR	Quantitative flow ratio
ROC	Receiver operating characteristic curves
TCFA	Thin-cap fibroatheroma
TVF	Target vessel failure

The incidence of in-stent restenosis (ISR) is currently rising by 1–2% per year[1,2]. Extensive studies of ISR treatment strategies have recommended the drug-coated balloon (DCB) as a Class I A treatment option[3]. However, adverse events continue to affect prognosis after DCB angioplasty, and effective methods for predicting these events are lacking, highlighting a significant issue.

The quantitative flow ratio (QFR), an innovative computational physiology tool based on three-dimensional anatomical reconstruction and hemodynamic simulation, has demonstrated strong correlation with the invasive wire flow reserve fraction (FFR), improving the diagnostic accuracy of functional stenosis identification through coronary angiography[4]. In contrast, optical coherence tomography (OCT) offers micron-scale resolution and exceptional lumen imaging capabilities, delivering unique insights into quantitative measurements and qualitative assessments[5,6]. However, the prognostic implications of the severity of physiological lesions assessed by QFR and neointimal characteristics evaluated by OCT remain unclear. This study aimed to explore the relationship between vessel-level QFR after DCB treatment for ISR and neointimal characteristics evaluated by OCT, along with their association with clinical outcomes.

Methods
Study design, population and study endpoints
This study is a single-center, retrospective, observational cohort study. Between January 2018 and March 2024, ISR is defined as a diameter narrowing of over 50% in the proximal or distal segments of the stent, as determined by angiography[2]. The exclusion criteria for this study included: poor angiographic image quality preventing QFR measurements, poor OCT image quality, lost OCT images and loss to follow-up. Ultimately, 204 diseased vessels from 204 patients with in-stent restenosis were included in the analysis (Supplemental Fig. 1). Baseline characteristics, QFR measurements before and after DCB angioplasty, OCT imaging prior to and following DCB angioplasty, and clinical follow-up data were analyzed. This study adhered to the ethical guidelines of the 1964 Declaration of Helsinki, received approval from the Ethics Committee of the Affiliated Hospital of Zunyi Medical University, and obtained written informed consent from all participants.

Clinical follow-up was conducted through outpatient visits, telephone contact, or structured follow-up. The primary outcome of the study was a target vessel failure (TVF), defined as a composite endpoint of cardiovascular death, target vessel myocardial infarction and target vessel revascularization according to the Academic Research Consortium-2 (ARC-2) consensus[7]. Further details regarding study endpoint definitions are provided in Supplemental Appendix 1.

Clinical baseline data, angiographic characteristics and percutaneous coronary nterventions (PCI) procedures
Clinical baseline data were collected from the hospital's electronic medical record system. This data consists of two main parts: (1) Demographic characteristics of the patients, including gender, age, blood pressure, body mass index, diabetes mellitus, smoking history, bleeding risk, hypertriglyceridemia, history of hypercholesterolemia, and peripheral artery disease. In addition, the patient's medication use after discharge was recorded. (2) Laboratory analysis included left ventricular ejection fraction and related hematological indicators, including white blood cell count, platelet count, triglycerides, total cholesterol, and markers of myocardial infarction. Details regarding angiographic and PCI procedures analysis are provided in Supplemental Appendix 1.

Off-line QFR computation
Calculating the QFR required uploading two angiographic images with angles of ≥ 25° to the AngioPlus software (Pulse Medical Imaging Technology, Shanghai, China) via a local network. Offline QFR calculations were performed using a previously described algorithm that included automatic depiction of the lumen contour by a thoroughly validated method. Manual corrections were allowed for cases where the angiographic image quality remained suboptimal after standard operating procedures (Fig. 1). In this study, a frame counting method was used to derive contrast flow rates from coronary angiograms for QFR calculation. QFR analysis was performed by well-trained technicians[8].

OCT image acquisition and analysis
All patients underwent OCT before and after DCB angioplasty. The procedure involved an intracoronary nitrate injection, followed by image acquisition using an OCT catheter (Dragonfly Duo, St. Jude Medical) and a frequency-domain OCT system (ILUMIEN OPTIS Intravessel-level Imaging System; St. Jude Medical, Inc., St. Paul, MN, USA). After delivering the OCT catheter along the guide wire to the distal part of the ISR lesion,
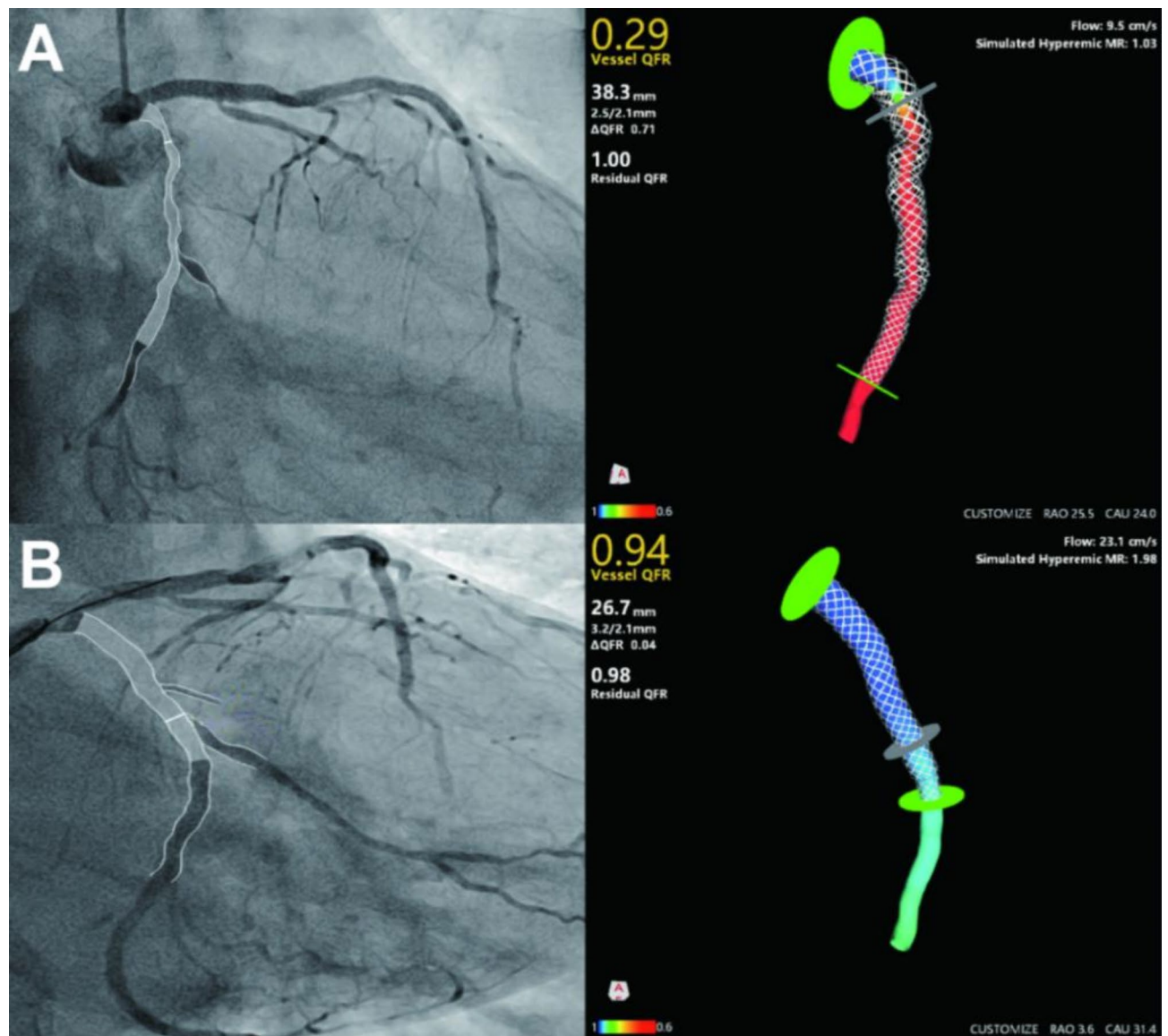
Fig. 1. QFR measurement before and after drug coated balloon angioplasty. (**A**) before drug coated balloon angioplasty; (**B**) after drug coated balloon angioplasty; *QFR* quantitative flow ratio.

it is advisable to advance beyond the stent segment and inject a contrast agent at a rate of 3–5 ml/s to replace the blood in the target vessel, facilitating a clear, blood-free environment for optimal imaging. The retraction and rotation rates were set to 18 mm/s and 100 frames/s, respectively. The total length of the OCT pullback is approximately 75 mm. To ensure optimal quality of the collected OCT images, the procedure was performed by an experienced interventional cardiologist. To ensure the accuracy of the OCT image analysis, two experienced clinicians, blinded to the baseline clinical and angiographic lesion characteristics, were selected for independent analysis. In cases of disagreement, a third independent clinician was consulted to reach a consensus[9]. For a detailed analysis of the quantitative and qualitative features of OCT, please refer to Supplemental Appendix 1, and the neointimal chaaracteristics of OCT are shown in Fig. 2.

Statistical analyses

To accurately assess the characteristics of the collected patient data, we classified the data into categorical and numerical variables. Categorical variables were presented as frequencies and percentages, and comparisons were made using the chi-square test or Fisher's exact test, when applicable. Continuous numerical variables were represented using different methods based on their distribution: normal distribution as mean ± standard deviation, and skewed distribution as median and interquartile range (IQR). Continuous numerical variables were compared between groups according to their distribution using the Student's t-test or Mann-Whitney U test. Additionally, receiver operating characteristic (ROC) curves were constructed to calculate the area under the curve and determine the optimal cut-off value for post-procedural QFR, assessing its predictive value for TVF after drug balloon angioplasty. The time to clinical outcome for each neointima and post-procedural QFR was
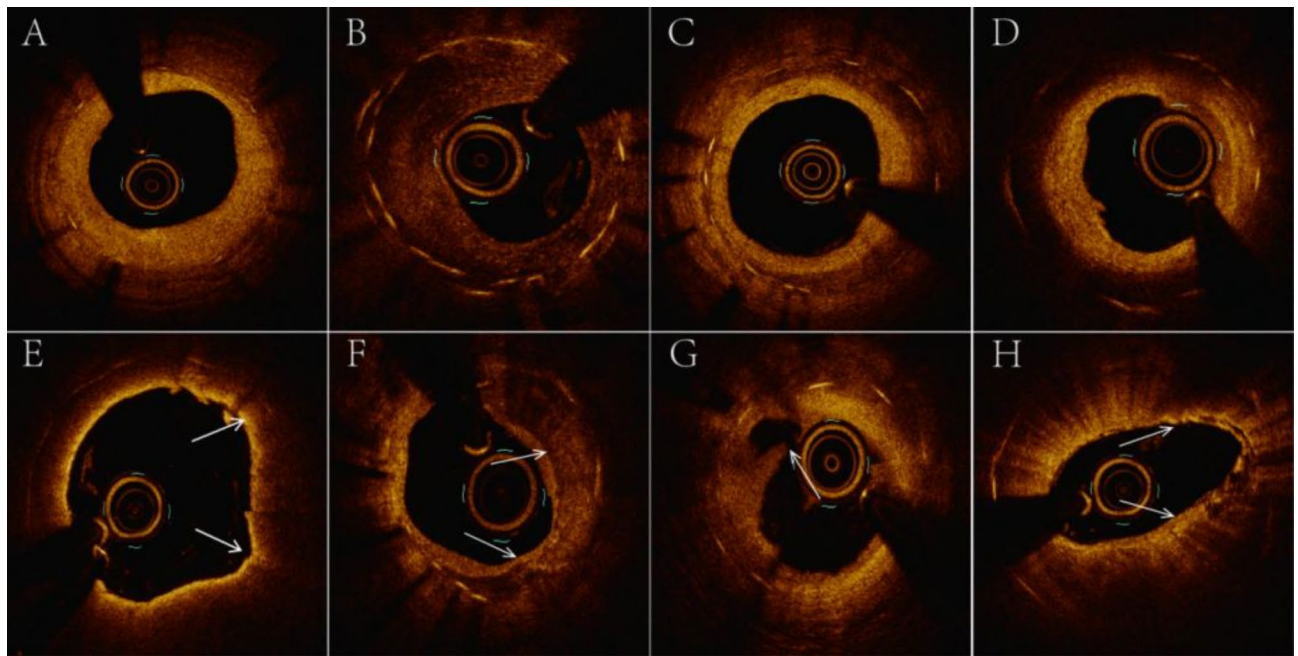
Fig. 2. Typical optical coherence tomography images of in-stent restenosis. (**A**) Homogeneous, (**B**) heterogeneous, (**C**) Layered, (**D**) in-stent neoatherosclerosis (ISNA), (**E**) thin-cap fibro-atheroma (TCFA), (**F**) calcification (arrows), (**G**) neointimal rupture (arrow), (**H**) macrophage infiltrates (arrow).

assessed using Kaplan-Meier survival curves, and event-free survival curves were compared with a log-rank test. Independent factors associated with TVF were identified through Cox regression analysis. Logistic regression was conducted to identify independent factors associated with low vessel-level QFR (below the optimal cut-off) following post-DCB angioplasty. Finally, to evaluate the additive value of pre-DCB angioplasty OCT findings and post-DCB angioplasty vessel-level QFR in identifying patients with subsequent TVF, we compared the improvement in the discriminatory and reclassification ability of models that included these factors against a model using only baseline characteristics. Data analysis for this study was conducted using SPSS software (version 29.0; IBM Corp, Armonk, NY, USA) and R version 4.2.3 (R Foundation for Statistical Computing, Vienna, Austria), employing a two-sided significance test with a threshold of $P < 0.05$.

Results
During a median follow-up of 756 days (IQR: 443.25, 1134.50), a total of 204 patients with ISR underwent OCT-guided DCB angioplasty. A total of 27 patients experienced TVF during the follow-up period. The specific distribution of TVF included: cardiovascular death (3 patients), target vessel myocardial infarction (8 patients) and target vessel revascularization (16 patients). Patients were classified into the TVF group ($n = 27$) and the non-TVF group ($n = 177$).

Comparisons between the TVF and non-TVF groups
Comparison of the data between the two groups at baseline revealed that the incidence of peripheral arterial disease was significantly higher in the TVF group than in the non-TVF group (5 [18.52%] vs. 7 [3.95%]; $P = 0.011$), and the remaining baseline characteristics were not significantly different between the two groups (Table 1).

In the comparison of angiographic characteristics, the rate of proximal segment lesions in the TVF group was significantly lower than that in the non-TVF group (4 [14.81%] vs. 74 [36.27%]; $P = 0.013$). After the DCB angioplasty, minimum lumen diameter in the TVF group (1.82 [IQR: 1.72, 2.10] vs. 2.04 [IQR: 1.81, 2.32]; $P = 0.040$), rate of diameter stenosis (28.90 [IQR: 21.15, 32.45] vs. 24.20 [IQR: 19.2, 27.80]; $P = 0.017$), area rate of stenosis (48.80 [IQR: 37.55, 55.50] vs. 42.30 [IQR: 34.60, 46.80]; $P = 0.013$) were all significantly lower than those in the non-TVF group. The post-procedural vessel-level QFR was compared between the two groups, the TVF group was significantly lower than the non-TVF group (0.89 [IQR: 0.87, 0.93] vs. 0.93 [IQR: 0.91, 0.96]; $P < 0.001$). And the vessel-level QFR improvement, also significantly lower in the TVF group than in the non-TVF group (0.10 [IQR: 0.07, 0.23] vs. 0.18 [IQR: 0.10, 0.38]; $P = 0.007$) (Table 2).

Table 3 summarizes the quantitative and qualitative results of DCB before and after angioplasty in ISR patients. In terms of quantitative characteristics, the proximal reference lumen diameter before DCB angioplasty in the TVF group was lower than that in the non-TVF group (2.85 [IQR: 2.70–3.11] vs. 3.13 [IQR: 2.86–3.33]; $P = 0.009$). Quantitative analysis of post-DCB angioplasty showed minimum lumen diameter in the TVF group (2.26 [IQR: 1.84–2.42] vs. 2.32 [IQR: 2.03, 2.59]; $P = 0.034$), Minimum lumen area (4.03 [IQR: 3.21, 5.04] vs. 4.65 [IQR: 3.78, 5.63]; $P = 0.040$), Maximum neointimal thickness (0.54 [IQR: 0.42, 0.72] vs. 0.38 [IQR: 0.31,

	TVF (n = 27)	Non-TVF (n = 177)	P value
Age, M (IQR), years	64 (56, 70)	62 (55, 69)	0.761
Male, n (%)	19 (70.37)	133 (75.14)	0.596
Heart rate, M (IQR), beats/min	75 (67.50, 83.00)	76 (68.00, 83.00)	0.947
Systolic blood pressure, M (IQR), mmHg	120 (113, 128)	127 (114, 138)	0.064
Diastolic blood pressure, M (IQR), mmHg	70 (66, 78)	74 (68, 83)	0.103
BMI, M (IQR), kg/m^2	23.50 (21.82, 25.64)	24.22 (22.35, 25.85)	0.546
Comorbidity, n (%)			
Hypertension, n (%)	14 (51.85)	111 (62.71)	0.281
Diabetes mellitus, n (%)	9 (33.33)	65 (36.72)	0.733
Hypertriglyceridemia, n (%)	13 (48.15)	83 (46.89)	0.903
Hypercholesterolemia, n (%)	8 (29.63)	42 (23.73)	0.507
Smoking history, n (%)	11 (40.74)	85 (48.02)	0.480
Chronic kidney disease, n (%)	4 (14.81)	24 (13.56)	1.000
Peripheralartery disease, n (%)	5 (18.52)	7 (3.95)	0.011
Previous stroke history, n (%)	2 (7.41)	8 (4.52)	0.866
Clinical presentation			
Stable ischemic heart disease, n (%)	15 (55.56)	73 (41.24)	0.162
Acute coronary syndrome, n (%)	12 (44.44)	104 (58.76)	0.162
Discharge therapy			
Aspirin, n (%)	21 (77.78)	144 (81.36)	0.660
Indobufen, n (%)	6 (22.22)	31 (17.51)	0.746
P2Y12 inhibitors			
Clopidogrel, n (%)	20 (74.07)	117 (66.10)	0.411
Ticagrelor, n (%)	7 (25.93)	56 (31.64)	0.550
Atorvastatin, n (%)	27 (100.00)	152 (85.88)	0.077
Rosuvastatin, n (%)	0 (0.00)	23 (12.99)	0.097
Ezetimibe Tablets, n (%)	2 (7.41)	30 (16.95)	0.324
PCSK9-inibitor, n (%)	2 (7.41)	37 (20.90)	0.097
Beta-blockers, n (%)	26 (96.30)	144 (81.36)	0.096
ACEI/ARB, n (%)	23 (85.19)	149 (84.18)	1.000
Calcium-channel blockers, n (%)	2 (7.41)	15 (8.47)	1.000
Laboratory results			
LVEF, M (IQR),	58.00 (42.50, 61.00)	58.00 (52.00, 61.00)	0.945
WBC count, M (IQR), ×10^9/L	7.35 (5.61, 8.71)	6.69 (5.45, 7.75)	0.293
Neutrophil count, M (IQR), ×10^9/L	7.35 (5.61, 8.71)	6.69 (5.45, 7.75)	0.293
Monocyte count, M (IQR), ×10^9/L	4.76 (3.37, 5.69)	4.26 (3.43, 5.30)	0.495
Lymphocyte count, M (IQR), ×10^9/L	0.56 (0.42, 0.61)	0.49 (0.37, 0.62)	0.288
Hb, M (IQR), g/L	1.52 (1.24, 1.83)	1.57 (1.17, 1.88)	0.755
Platelet count, ×10^9/L	137.00 (126.50, 152.00)	141.00 (129.00, 152.00)	0.923
RBC count, M (IQR), ×10^{12}/L	191.00 (148.00, 218.00)	193.00 (154.00, 240.00)	0.342
RBC distribution, M (IQR)	4.35 (4.21, 5.13)	4.63 (4.13, 5.02)	0.765
ApolipoproteinA1, M (IQR), g/L	1.23 (1.10, 1.35)	1.20 (1.10, 1.35)	0.976
ApolipoproteinB, M (IQR), g/L	0.69 (0.57, 0.93)	0.74 (0.58, 0.92)	0.587
Triglycerides, M (IQR), mmol/L	1.72 (1.17, 2.36)	1.65 (1.19, 2.67)	0.608
Total cholesterol, M (IQR), mmol/L	3.83 (3.54, 4.95)	3.96 (3.30, 4.86)	0.896
HDL-C, M (IQR), mmol/L	1.12 (0.95, 1.25)	1.05 (0.91, 1.21)	0.379
LDL-C, M (IQR), mmol/L	2.33 (1.88, 2.93)	2.28 (1.89, 2.87)	0.883
Myoglobin, M (IQR), ng/ml	29.00 (21.50, 45.00)	31.00 (21.00, 45.00)	0.814
Continued			

	TVF (n = 27)	Non-TVF (n = 177)	P value
Hs-cTn, M (IQR), ng/ml	11.25 (7.00, 24.67)	14.75 (8.84, 26.15)	0.374
Uric acid, M (IQR), mmol/L	347 (314.50, 375.50)	358 (322, 437)	0.321
Urea, M (IQR), mmol/L	5.57 (4.72, 7.32)	6.10 (4.90, 7.30)	0.436
Creatinine, M (IQR), µmmol/L	77.00 (66.50, 99.50)	85.00 (71.00, 101.00)	0.356
BNP, M (IQR), ng/L	157.00 (90.50, 680.10)	167.00 (66.00, 618.05)	0.568

Table 1. Baseline clinical and laboratory characteristics. *TVF* target vessel failure, *M (IQR)* median (interquartile range), *BMI* body mass index, *PCSK9-inibitor* proprotein convertase subtilisin/kexin type 9 inibitor, *ACEI* angiotensin-converting enzyme inhibitor, *ARB* angiotensin receptor blocker, *LVEF* left ventricular ejection fraction, *WBC* white blood cell, *Hb* haemoglobin, *RBC* red blood cell, *HDL-C* high-density lipoprotein cholesterol, *LDL-C* low-density lipoprotein cholesterol, *Hs-cTn* high-sensitivity cardiac troponin, *BNP* brain natriuretic peptide.

0.49]; $P < 0.001$), Improvement in maximal neointimal thickness (0.55 [IQR: 0.38, 0.70] vs. 0.70 [IQR: 0.52, 0.89]; $P = 0.004$) were all significantly lower than those in the non-TVF group. According to the analysis of qualitative characteristics of in-stent restenosis lesions, the incidence of heterogeneous neointima (13 [48.15%] vs. 32 [18.08%]; $P < 0.001$) was significantly higher compared with the non-TVF group (Supplemental Fig. 2). In addition, the incidence of thin-cap fibroatheroma (6 [22.22%] vs. 11 [6.21%]; $P = 0.015$), neointimal rupture (7 [25.93%] vs. 13 [7.34%]; $P = 0.007$) were significantly higher than those in the non-TVF group.

Factors associated with TVF
The results of the univariable and multivariable Cox regression analyses for TVF are presented in Table 4. Variables with $P < 0.1$ in the univariable analysis were included in the multivariable Cox regression analysis. The multivariable model indicated that monocyte count, proximal lesional segment, post-procedural vessel-level QFR, and heterogeneous neointima were independently associated with TVF.

Among the factors independently associated with TVF, post-procedural vessel-level QFR and heterogeneous neointima are the most critical. Receiver operating characteristic curve analysis revealed that the cutoff value of vessel-level QFR for identifying patients with subsequent TVF was 0.895 (sensitivity: 52%; specificity: 88%; area under the curve: 0.738; 95% confidence interval: 0.629–0.847; $p < 0.0001$; Supplemental Fig. 3). The incidence of TVF was 6.51 times higher in vessels with low vessel-level QFR (≤ 0.895) compared to those with high vessel-level QFR (> 0.895) (95%CI [2.21–19.91]; log-rank $P < 0.0001$; Supplemental Fig. 4). The cumulative TVF rate analysis showed that the incidence of TVF in heterogeneous neointima was significantly higher than in the other three types of neointima (log-rank $P = 0.0024$; Supplemental Fig. 5A). These three types were classified as non-heterogeneous neointima. The incidence of TVF in heterogeneous neointima was 3.80 times higher than in non-heterogeneous neointima (95%CI [1.47–9.83]; log-rank $P = 0.0015$; Supplemental Fig. 5B). The TVF rate was highest in vessels with both features, followed by those with one feature and those without either feature (Fig. 3A). The TVF rate in vessels with both features was 10.69 times higher than in all other vessels (95% CI [2.05–55.79]; log-rank $P < 0.0001$) (Fig. 3B).

Factors associated with low vessel-level QFR (≤ 0.895)
Multivariable logistic regression analysis revealed that post-procedural maximum neointimal thickness (OR: 0.016, 95% CI [0.003–0.84]; $P < 0.001$), improvement in the maximal neointimal thickness (OR: 0.003, 95% CI [0.00–0.06]; $P < 0.001$) and heterogeneous neointima (OR: 3.60, 95% CI [1.03–12.60]; $P = 0.045$) were independently associated with low vessel-level QFR (≤ 0.895) (Supplemental Table 1).

Incremental value of vessel-level QFR in identifying patients with subsequent TVF
Figure 4 presents the C-index, net reclassification index, and relative integrated discrimination improvement values for the three models. In comparison to model 1 (monocyte count and proximal lesional segment), model 2 (model 1 plus pre-procedural OCT findings) demonstrated significantly greater discriminatory ability (C-index: 0.714 vs. 0.624; $P = 0.048$) and reclassification ability (net reclassification index: 0.387; $P = 0.036$; relative integrated discrimination improvement: 0.103; $P = 0.008$) for identifying patients with subsequent TVF. Compared to model 2, model 3 (model 2 plus pre-procedural vessel-level QFR) exhibited an even greater discriminatory ability (C-index: 807 vs. 0.714; $P = 0.025$) and incremental reclassification ability (net reclassification index: 0.588; $P = 0.003$; relative integrated discrimination improvement: 0.085; $P = 0.048$).

Discussion
The main findings of this study are as follows: (1) Post-procedural vessel-level QFR and heterogeneous neointima observed via OCT were independent predictors of TVF after DCB angioplasty in patients with ISR. (2) Vessel-level QFR was significantly lower in the TVF group compared to the non-TVF group following DCB angioplasty in patients with ISR. (3) The optimal cut-off value for predicting QFR in TVF is 0.895; additionally, post-procedural maximum neointimal thickness, improvement in the maximal neointimal thickness and heterogeneous neointima were independently associated with low vessel-level QFR (≤ 0.895). (4) The incidence of TVF in ISR patients with low vessel-level QFR and heterogeneous neointima after DCB angioplasty is 10.69 times higher than that in all other vessels. (5) Vessel-level QFR post-DCB angioplasty in patients with ISR

	TVF (n = 27)	Non-TVF (n = 177)	*P* value
Angiographic features			
Multivessel disease, n (%)	22 (81.48)	127 (71.75)	0.289
ISR location			0.519
LAD, n (%)	17 (62.96)	103 (58.19)	0.639
LCX, n (%)	1 (3.70)	19 (10.73)	0.425
RCA, n (%)	9 (33.33)	55 (31.07)	0.814
Lesional segment			0.036
Proximal, n (%)	74 (36.27)	4 (14.81)	0.013
Middle, n (%)	102 (50.00)	17 (62.96)	0.148
Distal, n (%)	28 (13.73)	6 (22.22)	0.281
Restenosis pattern			0.511
Mehran I, n (%)	26 (12.75)	1 (3.70)	0.229
Mehran II, n (%)	91 (44.61)	13 (48.15)	0.691
Mehran III, n (%)	59 (28.92)	9 (33.33)	0.587
Mehran IV, n (%)	28 (13.73)	4 (14.81)	1.000
Pre-DCB angioplasty QCA			
Reference vessel diameter, M (IQR), mm	2.58 (2.42, 2.81)	2.61 (2.39, 2.94)	0.471
Minimal lumen diameter, M (IQR), mm	1.05 (0.94, 1.34)	1.16 (0.92, 1.38)	0.703
Diameter stenosis rate, M (IQR), %	54.00 (50.00, 61.65)	53.70 (49.70, 62.30)	0.992
Area stenosis, M (IQR), %	78.60 (71.15, 83.85)	77.60 (71.70, 85.40)	0.619
Lesion length, M (IQR), mm	21.16 (16.11, 24.28)	18.49 (13.33, 22.94)	0.195
Post-DCB angioplasty QCA			
Minimal lumen diameter, M (IQR), mm	1.82 (1.72, 2.10)	2.04 (1.81, 2.32)	0.040
Diameter stenosis rate, M (IQR), %	28.90 (21.15, 32.45)	24.20 (19.20, 27.80)	0.017
Area stenosis rate, M (IQR), %	48.80 (37.55, 55.50)	42.30 (34.60, 46.80)	0.013
Acute lumen gain, M (IQR), mm	0.80 (0.59, 0.93)	0.87 (0.66, 1.12)	0.095
Pre-DCB angioplasty data:			
Predilation, M (IQR), atm	13.00 (11.00, 14.00)	13.00 (12.00, 15.00)	0.690
DCB length, M (IQR), mm	26.00 (22.50, 30.00)	25.00 (20.00, 30.00)	0.151
DCB diameter, M (IQR), mm	3.00 (2.75, 3.00)	3.00 (2.75, 3.50)	0.234
DCB pressure, M (IQR), atm	10.00 (8.00, 12.00)	10.00 (8.00, 12.00)	0.413
DCB Inflation time, M (IQR), s	60.00 (60.00, 70.00)	60.00 (60.00, 70.00)	0.958
Procedural time, M (IQR), min	90 (74, 108)	90 (72, 113)	0.961
Contrast agent, M (IQR), ml	250 (200 300)	240 (200, 300)	0.654
Pre-DCB angioplasty TIMI flow grade, M (IQR)	3.00 (3.00, 3.00)	3.00 (3.00, 3.00)	0.382
Vessel-level QFR			
Pre-DCB angioplasty QFR, M (IQR)	0.79 (0.66, 0.82)	0.76 (0.56, 0.81)	0.156
Post-DCB angioplasty QFR, M (IQR)	0.89 (0.87, 0.93)	0.93 (0.91, 0.96)	< 0.001
QFR improvement, M (IQR)	0.10 (0.07, 0.23)	0.18 (0.10, 0.38)	0.007

Table 2. Baseline angiographic, and procedural characteristics. *TVF* target vessel failure, *ISR* in-stent restenosis, *LAD* left anterior descending artery, *LCX* left circumflex artery, *RCA* right coronary artery, *DCB* drug-coated balloon, *QCA* quantitative coronary angiography, *M (IQR)* median (interquartile range), *TIMI* thrombolysis in myocardial infarction, *QFR* quantitative flow ratio.

provides additional predictive value beyond morphological OCT outcomes for identifying patients at risk for subsequent TVF.

DCB angioplasty is one of the most effective therapeutic strategies for ISR and exemplifies the concept of intervention without stent placement. The mechanism involves using a balloon coated with an antiproliferative drug, which is inflated at the lesion site under specific pressure. This process allows for rapid and uniform transfer of the drug through the lipophilic matrix into the vessel wall, eliminating the need for a permanent implant[10]. Consequently, the duration of dual antiplatelet therapy is shortened, and the risk of chronic inflammation in the vessel wall is reduced, thereby minimizing the risks of bleeding and revascularization. However, adverse clinical events following DCB angioplasty cannot be overlooked, highlighting the need for appropriate predictive indicators to optimize DCB strategies.

Currently, FFR is the gold standard for determining the need for PCI in patients with coronary artery disease. Previous studies have demonstrated an inverse relationship between post-PCI FFR and future adverse cardiac events. The accepted FFR cut-off for identifying a hemodynamic-related lesion is 0.8[3]. However, the disadvantages

	TVF (n = 27)	Non-TVF (n = 177)	P value
Quantitative variables			
Pre-DCB angioplasty			
Distal reference vessel diameter, M (IQR), mm	2.41 (2.20, 2.74)	2.56 (2.25, 2.88)	0.406
Proximal reference vessel diameter, M (IQR), mm	2.85 (2.70, 3.11)	3.13 (2.86, 3.33)	0.009
Minimal luminal diameter, M (IQR), mm	1.28 (1.04, 1.52)	1.38 (1.15, 1.61)	0.203
Minimal luminal area, M (IQR), mm^2	1.59 (0.96, 2.00)	1.69 (1.29, 2.15)	0.327
Area stenosis rate, M (IQR), %	72.70 (66.25, 82.40)	73.30 (68.20, 80.10)	0.858
Lesion length, M (IQR), mm	21.20 (16.80, 25.10)	18.60 (13.60, 22.80)	0.072
Maximal neointimal thickness, M (IQR), mm	1.13 (0.89, 1.35)	1.13 (0.96, 1.31)	0.722
Post-DCB angioplasty			
Minimal luminal diameter, M (IQR), mm	2.26 (1.84, 2.42)	2.32 (2.03, 2.59)	0.034
Acute lumen gain, M (IQR), mm	0.79 (0.58, 1.02)	0.94 (0.68, 1.16)	0.072
Minimal luminal area, M (IQR), mm^2	4.03 (3.21, 5.04)	4.65 (3.78, 5.63)	0.040
Maximal neointimal thickness, M (IQR), mm	0.54 (0.42, 0.72)	0.38 (0.31, 0.49)	< 0.001
Maximal neointimal thickness improvement, M (IQR), mm	0.55 (0.38, 0.70)	0.70 (0.52, 0.89)	0.004
Qualitative variables			
Neointimal characteristics			0.005
Homogeneous, n (%)	6 (22.22)	67 (37.85)	0.115
Heterogeneous, n (%)	13 (48.15)	32 (18.08)	< 0.001
Layered, n (%)	5 (18.52)	39 (22.03)	0.679
Neoatherosclerosis, n (%)	3 (11.11)	39 (22.03)	0.191
Thin-cap fibroatheroma, n (%)	6 (22.22)	11 (6.21)	0.015
Calcified plaque, n (%)	3 (11.11)	7 (3.95)	0.260
Neointimal rupture, n (%)	7 (25.93)	13 (7.34)	0.007
Macrophage infiltration, n (%)	7 (25.93)	21 (11.86)	0.093

Table 3. Optical coherence tomography characteristics. *TVF* target vessel failure, *DCB* drug-coated balloon, *M (IQR)* median (interquartile range).

of FFR, including its invasive nature and the requirement for pharmacologically induced congestion, contribute to higher costs and result in its underutilization in clinical practice. To address these limitations, QFR was developed to facilitate the calculation of functional parameters more simply and rapidly[11]. Studies have shown a strong correlation and consistency between QFR and FFR, using FFR as the reference standard[12,13]. The recently published FAVOR III Europe study indicates that the QFR-guided strategy is inferior to the FFR-guided strategy. However, the correlation and consistency between the two strategies are evident[14]. These indicate that QFR has significant potential for prognostic assessment, making it crucial to measure QFR values after PCI. A study by Biscaglia et al.[15] showed that low QFR values after PCI are independent predictors of adverse events, establishing an optimal cut-off of 0.89 for QFR after PCI. Similarly, research by Ki et al.[16] and others demonstrated that lesions with low QFR (< 0.90) are associated with a significantly higher risk of adverse events. Since none of these studies focused on ISR lesions, Liontou et al.[17] examined the diagnostic performance of QFR in ISR lesions, using FFR as a reference standard, and found that QFR exhibited high diagnostic performance similar to that of primary lesions. The application of post-procedural physiological assessment was subsequently extended to DCB angioplasty in ISR lesions, with clinical outcomes analyzed yielding consistent results[18,19]. Our study also reconfirmed these findings, with optimal cut-off values aligning with previous research. Unlike FFR, QFR can be computed using only quantitative lumen information from angiographic images to derive virtual FFR. Therefore, QFR values for ISR lesions after DCB angioplasty are straightforward, efficient, and feasible for predicting clinical adverse events.

OCT is a well-established method for imaging intracoronary structures. Unlike conventional angiography, which provides only basic information about the shape of the vessel lumen without insight into the inner wall, OCT addresses this limitation by offering a comprehensive view of the diseased vessel's inner wall. It provides detailed tomographic or cross-sectional images of the coronary arteries, including data on the lumen, vessel wall, plaque burden, and the composition and distribution of plaque. This advancement has significantly improved the prognosis for patients undergoing PCI[20,21]. This method has been utilized to characterize the vessel-level responses following PCI, thereby enhancing our understanding of the development of ISR. Recently, the neointima in ISR lesions identified via OCT has been primarily categorized into homogeneous, heterogeneous, layered neointima, and neoatherosclerosis[22,23]. Previous research has demonstrated a significant correlation between the chosen treatment approach and neointima patterns, highlighting the superiority of drug-eluting stents (DES) over DCB in cases of heterogeneous neointima[24,25]. This study further confirmed the poorer prognosis associated with DCB for treating heterogeneous neointima. Previous studies have shown that neointimal abnormalities, such as fibrin deposition or intimal hyperplasia, are commonly observed in heterogeneous neointima[26,27]. These

	Univariable regression			Multivariable regression		
	HR	95% CI	P value	HR	95% CI	P value
Systolic blood pressure	0.98	0.96–1.00	0.063			
Diastolic blood pressure	0.97	0.93–1.00	0.080			
Peripheralartery disease	0.23	0.09–0.61	0.032			
Monocyte count	4.82	0.99–23.41	0.003	7.72	1.68–35.99	0.009
Lesional segment						
Proximal	3.96	1.36–11.49	0.011	0.24	0.08–0.69	0.008
Pre-procedural QCA						
Reference vessel diameter	0.63	0.25–1.56	0.322			
Post-procedural QCA						
Minimal lumen diameter	0.32	0.10–1.04	0.058			
Diameter stenosis rate	1.06	1.00–1.11	0.032			
Area stenosis rate	1.05	1.01–1.09	0.021			
Physiological results						
Post-DCB angioplasty QFR (per 0.1 increase)	0.06	0.02–0.18	< 0.001	0.11	0.03–0.41	0.001
OCT quantitative variables						
Post-DCB angioplasty						
Proximal reference vessel diameter	0.26	0.10–0.64	0.003			
Minimal luminal diameter	0.26	0.09–0.77	0.015			
Minimal luminal area	0.72	0.52–1.00	0.049			
Maximal neointimal thickness	24.11	5.29–109.81	< 0.001			
Maximal neointimal thickness improvement	0.08	0.01–0.41	0.003			
Qualitative variables						
Neointimal characteristics						
Homogeneous	1.88	0.76–4.66	0.174			
Heterogeneous	0.26	0.12–0.56	0.001	2.95	1.29–6.71	0.01
Thin-cap fibroatheroma	0.35	0.14–0.88	0.026			
Neointimal rupture	0.36	0.13–1.01	0.051			
Macrophage infiltration	0.49	0.21–1.17	0.109			

Table 4. Cox regression analyses for factors associated with TVF after DCB in patients with ISR. *TVF* target vessel failure, *DCB* drug-coated balloon, *ISR* in-stent restenosis, *HR* hazard ratio, *CI* confidence interval, *QCA* quantitative coronary angiography, *QFR* quantitative flow ratio, *OCT* optical coherence tomography.

abnormal inflammatory reactions contribute to adverse clinical outcomes and may underlie the poor prognosis of DCB treatment in such cases.

Recently, incorporating physiological indicators derived from hemodynamics alongside the morphological characteristics observed by OCT for combined prediction has shown to significantly enhance the predictive ability for clinical outcomes[16,28]. Furthermore, our research strongly supports the applicability of this combined predictor in cases of ISR lesions treated with DCB. To validate the practicality of this finding, further prospective studies with larger sample sizes are recommended.

Study limitations
This study is a retrospective analysis conducted at a single center, which inherently includes limitations associated with its design. First, we excluded patients with poor-quality angiography and OCT images, leading to unavoidable selection bias. Second, the primary outcome of interest, TVF is a composite outcome, and the factors associated with it may differ across various clinical outcomes. Due to the relatively small sample size, we are unable to evaluate each clinical outcome separately and cannot ascertain any differences between them. Third, the study is a post-hoc analysis, and the QFR computation was performed offline, which may affect the accuracy of the QFR values. However, previous studies have demonstrated good consistency between offline and online measurements. Finally, the results of this study should be regarded as exploratory; further prospective studies are needed to determine whether physiological methods based on QFR and morphological methods based on OCT can improve clinical outcomes for patients receiving DCB treatment for ISR.

Conclusions
This study demonstrated that vessel-level QFR and heterogeneous neointima were independent factors associated with TVF in ISR patients after DCB angioplasty. Incorporating QFR measurements alongside OCT findings enhances the ability to discriminate patients at risk for subsequent TVF after DCB angioplasty for ISR.
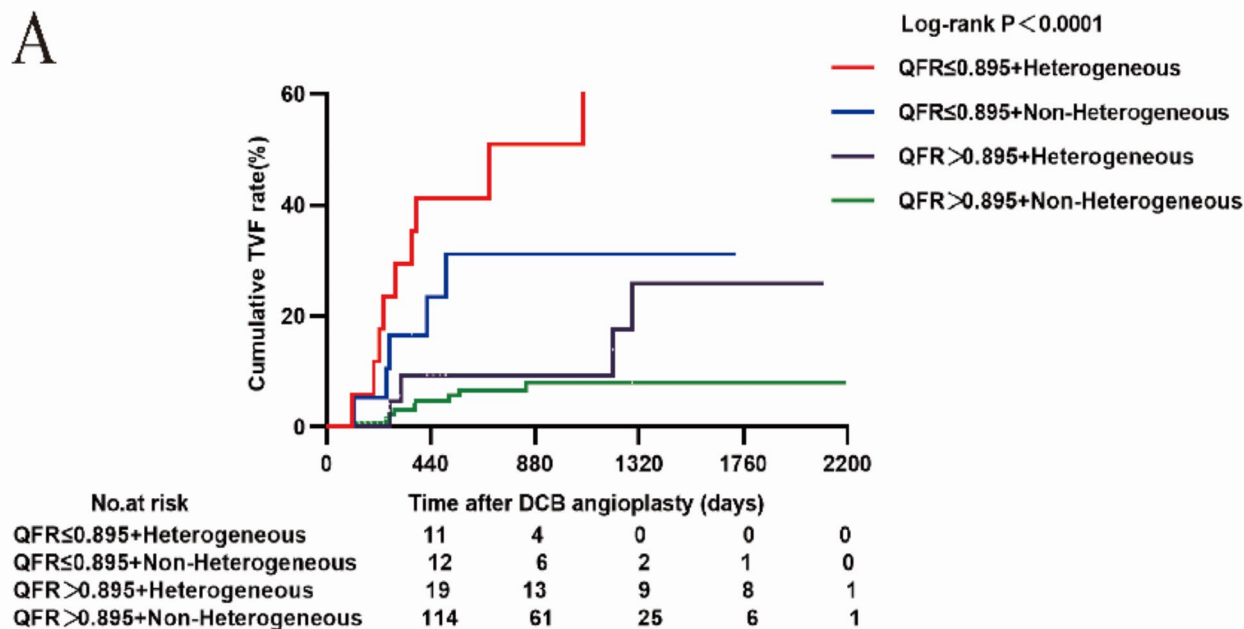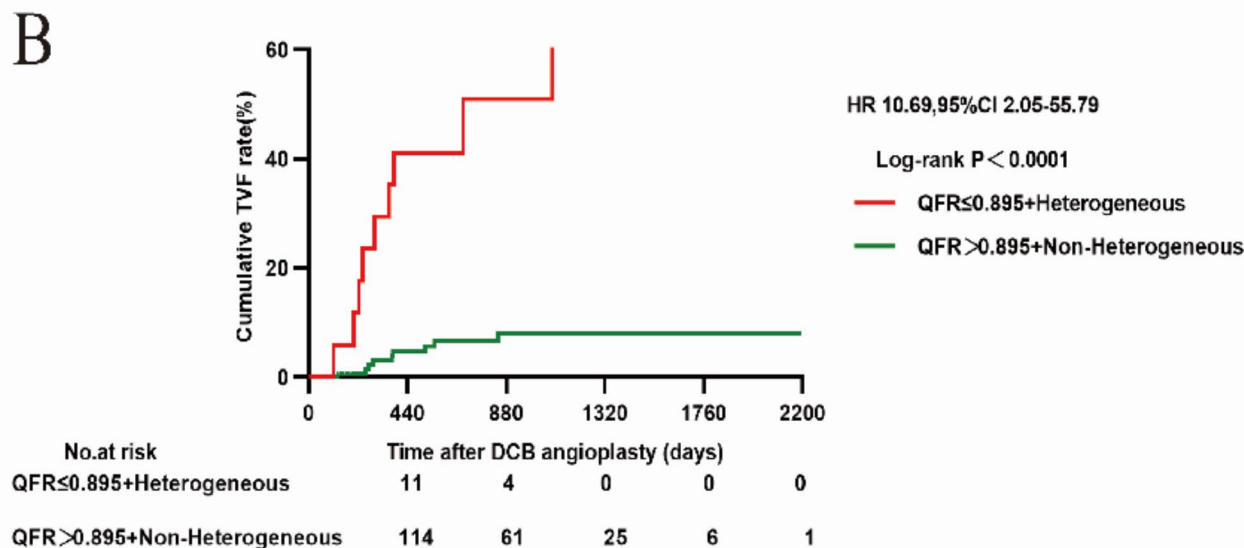
Fig. 3. Kaplan–Meier curves of TVF according to low vessel-level QFR combined with the Presence of heterogeneous neointimal pattern in ISR (**A,B**). *P* values were calculated using the log-rank test. *TVF* target vessel failure, *QFR* quantitative flow ratio, *HR* hazard ratio, *CI* confidence interval.
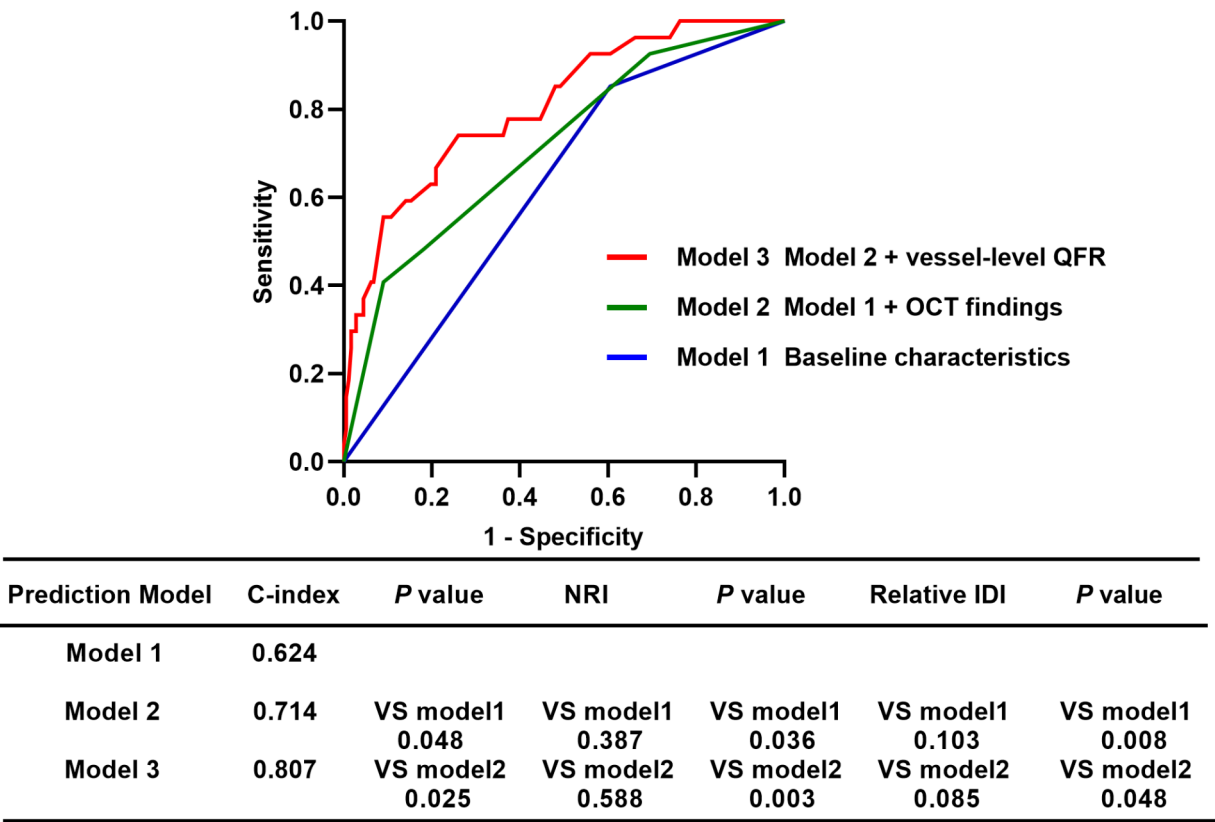
Prediction Model	C-index	P value	NRI	P value	Relative IDI	P value
Model 1	0.624					
Model 2	0.714	VS model1 0.048	VS model1 0.387	VS model1 0.036	VS model1 0.103	VS model1 0.008
Model 3	0.807	VS model2 0.025	VS model2 0.588	VS model2 0.003	VS model2 0.085	VS model2 0.048

Fig. 4. Discriminatory ability of predictive models for TVF. *TVF* target vessel failure, *OCT* optical coherence tomography, *QFR* quantitative flow ratio, *IDI* integrated discrimination improvement, *NRI* net reclassification index.

Data availability

Due to privacy and ethical constraints, the datasets generated and analysed in this study are not publicly available but can be obtained from the corresponding author.

References
1. Madhavan, M. V. et al. Stent-related adverse events >1 year after percutaneous coronary intervention. *J. Am. Coll. Cardiol.* **75**, 590–604 (2020).
2. Giustino, G. et al. Coronary in-stent restenosis: JACC state-of-the-art review. *J. Am. Coll. Cardiol.* **80**, 348–372 (2022).
3. Neumann, F.-J. et al. 2018 ESC/EACTS guidelines on myocardial revascularization. *Eur. Heart J.* **40**, 87–165 (2019).
4. Tu, S. et al. Diagnostic accuracy of fast computational approaches to derive fractional flow reserve from diagnostic coronary angiography: The international multicenter FAVOR pilot study. *JACC Cardiovasc. Interv.* **9**, 2024–2035 (2016).
5. Han, Y. et al. OCT analysis of in-stent neointima over 5 years post-DES implantation. *Zhonghua Xin Xue Guan Bing Za Zhi* **52**, 150–157 (2024).
6. Gonzalo, N. et al. Optical coherence tomography patterns of stent restenosis. *Am. Heart J.* **158**, 284–293 (2009).
7. Garcia-Garcia, H. M. et al. Standardized end point definitions for coronary intervention trials: The academic research consortium-2 consensus document. *Eur. Heart J.* **39**, 2192–2207 (2018).
8. Xu, B. et al. Diagnostic accuracy of angiography-based quantitative flow ratio measurements for online assessment of coronary stenosis. *J. Am. Coll. Cardiol.* **70**, 3077–3087 (2017).
9. Tearney, G. J. et al. Consensus standards for acquisition, measurement, and reporting of intravascular optical coherence tomography studies: A report from the International Working Group for intravascular optical coherence tomography standardization and validation. *J. Am. Coll. Cardiol.* **59**, 1058–1072 (2012).
10. Jeger, R. V. et al. Drug-coated balloons for coronary artery disease: Third report of the international DCB Consensus Group. *JACC Cardiovasc. Interv.* **13**, 1391–1402 (2020).
11. Cerrato, E. et al. Quantitative flow ratio as a new tool for angiography-based physiological evaluation of coronary artery disease: A review. *Future Cardiol.* **17**, 1435–1452 (2021).
12. Yang, W. T., Shen, L. H. & He, B. Research update on the validation, comparison and clinical application of quantitative flow ratio. *Zhonghua Xin Xue Guan Bing Za Zhi* **50**, 302–308 (2022).
13. Chen, H. et al. Prognostic value of quantitative flow ratio in patients with coronary heart disease after percutaneous coronary intervention therapy: A meta-analysis. *Front. Cardiovasc. Med.* **10**, 1164290 (2023).

14. Andersen, B. K. et al. Quantitative flow ratio versus fractional flow reserve for coronary revascularisation guidance (FAVOR III Europe): A multicentre, randomised, non-inferiority trial. *Lancet* **404**, 1835–1846 (2024).
15. Biscaglia, S. et al. Prognostic value of QFR measured immediately after successful stent implantation: The international multicenter prospective HAWKEYE study. *JACC Cardiovasc. Interv.* **12**, 2079–2088 (2019).
16. Ki, Y.-J. et al. Prognostic implications of quantitative flow ratio and plaque characteristics in intravascular ultrasound-guided treatment strategy. *JACC Cardiovasc. Interv.* **17**, 461–470 (2024).
17. Liontou, C. et al. Quantitative flow ratio for functional evaluation of in-stent restenosis. *EuroIntervention* **17**, e396–e398 (2021).
18. Cai, X. et al. Prognostic value of quantitative flow ratio measured immediately after drug-coated balloon angioplasty for in-stent restenosis. *Catheter. Cardiovasc. Interv.* **97**(Suppl 2), 1048–1054 (2021).
19. Tang, J. et al. Clinical implication of quantitative flow ratio to predict clinical events after drug-coated balloon angioplasty in patients with in-stent restenosis. *Clin. Cardiol.* **44**, 978–986 (2021).
20. Hasan, S. M., Faluk, M., Patel, J. D., Abdelmaseih, R. & Patel, J. Use of optical coherence tomography in coronary artery disease: Review article. *Curr. Probl. Cardiol.* **46**, 100597 (2021).
21. Mintz, G. S., Matsumura, M., Ali, Z. & Maehara, A. Clinical utility of intravascular imaging: Past, present, and future. *JACC Cardiovasc. Imaging* **15**, 1799–1820 (2022).
22. Lutter, C. et al. Histopathological differential diagnosis of optical coherence tomographic image interpretation after stenting. *JACC Cardiovasc. Interv.* **9**, 2511–2523 (2016).
23. Kim, H. O. et al. Neointima characteristics as a prognostic marker for drug-coated balloon angioplasty in patients with in-stent restenosis: An optical coherence tomography study. *Coron Artery Dis.* **31**, 694–702 (2020).
24. Xhepa, E. et al. Clinical outcomes by optical characteristics of neointima and treatment modality in patients with coronary in-stent restenosis. *EuroIntervention* **17**, e388–e395 (2021).
25. Lee, J.-H. et al. Different neointimal pattern in early vs. late in-stent restenosis and clinical outcomes after drug-coated balloon angioplasty-an optical coherence tomography study. *Circ. J.* **82**, 2745–2752 (2018).
26. Lee, S. Y., Hong, M. K. & Jang, Y. Formation and transformation of neointima after drug-eluting stent implantation: Insights from optical coherence tomographic studies. *Korean Circ. J.* **47**, 823–832 (2017).
27. Kim, J.-S. et al. Long-term outcomes of neointimal hyperplasia without neoatherosclerosis after drug-eluting stent implantation. *JACC Cardiovasc. Imaging* **7**, 788–795 (2014).
28. Kakizaki, S. et al. Optical coherence tomography fractional flow reserve and cardiovascular outcomes in patients with acute coronary syndrome. *JACC Cardiovasc. Interv.* **15**, 2035–2048 (2022).

Author contributions
Zhenglong Wang and Bei Shi conceived the study. Shiwan Lu, Li Pan and Ning Gu did the OCT analysis. Yi Deng, Chancui Deng, Xiushi Li and Feng Wang performed the statistical analysis and interpreted the study results. Shiwan Lu wrote the first draft of the manuscript, which was critically revised for important intellectual content by Yongchao Zhao. All authors read and approved the final manuscript.

Declarations

Competing interests
The authors declare no competing interests.

Ethical approval
The protocol was approved by the Ethics Committee of the Affiliated Hospital of Zunyi Medical University.

Consent to participate
Informed consent was obtained from all individual participants included in the study.

Additional information
Supplementary Information The online version contains supplementary material available at https://doi.org/10.1038/s41598-024-83748-y.

Correspondence and requests for materials should be addressed to Z.W. or B.S.

Reprints and permissions information is available at www.nature.com/reprints.

Publisher's note Springer Nature remains neutral with regard to jurisdictional claims in published maps and institutional affiliations.